ACS APPLIED MATERIALS & INTERFACES

RESEARCH ARTICLE

www.acsami.org

Polydopamine/Liposome Coatings and Their Interaction with Myoblast Cells

Martin E. Lynge, Ryosuke Ogaki, Anja Overgård Laursen, Jette Lovmand, Duncan S. Sutherland, and Brigitte Städler*

iNANO Interdisciplinary Nanoscience Centre, Aarhus University, Denmark

Supporting Information

ABSTRACT: Surface-mediated drug delivery is a recent concept, where active surface coatings are employed to deliver therapeutic cargo to cells. Herein, we explore the potential of liposomes embedded in polydopamine (PDA) coatings to serve as drug deposits stored on planar substrates. We quantify the PDA growth rate on glass by XPS and show that PDA coatings support myoblast adherence and proliferation. Further, PDA capping layers were deposited on glass substrates precoated with poly(L-lysine) and zwitterionic liposomes. Already thin PDA capping layers render liposome coated surfaces cell adhesive. We experimentally show for the first time, the internalization of a model hydrophobic cargo, that is, fluorescent lipids embedded within the lipid bilayer of liposomes by the cells from the surface. This is evident from the fluorescence exhibited by the cells grown on PDA coatings containing fluorescently labeled liposomes, with the highest fluorescent intensity found in the close proximity of the cell nuclei. The cargo uptake efficiency depends on the thickness of the PDA capping layer and the cell residence time on the coated substrates. Taken together, we demonstrate the first step toward the establishment of a versatile approach using liposomal drug deposits in polymer thin films for surface-mediated drug delivery.

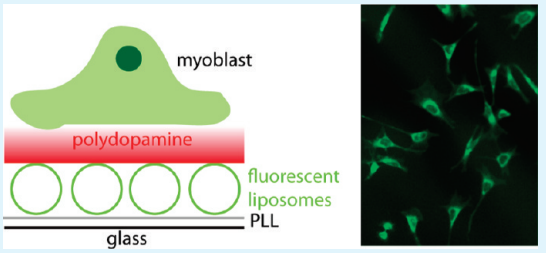

KEYWORDS: surface-mediated drug delivery, liposomes, polydopamine, myoblasts, flow cytometry, X-ray photoelectron spectroscopy

INTRODUCTION

Smart drug delivery vehicles and appropriated administration routes are among the predominant factors that have enabled increasing performance of drugs or opened possibilities for novel future medical treatments. Recently, an alternative approach to the more traditional solution-based drug delivery, namely surface-mediated drug delivery, has attracted increasing interest as a novel drug administration concept. The basic idea involves the assembly of functional cell-adhesive films on surfaces allowing a well controlled cellular access to the embedded cargo, for example, drug-eluting stents.

Multilayered thin films deposited via the sequential assembly of interacting polymers, have shown particular promise as functional coatings for surface-mediated drug delivery.[1] These films offer a high degree of control over their properties, for example, the type and number of assembled building blocks governs the softness, surface charge, or cell adhesive/repellent characteristics. The delivery of low molecular weight drugs,[2,3] peptides,[4] proteins,[5−7] or DNA[8,9] from such thin films to a variety of cell types has been demonstrated. Further, macromolecular assemblies such as dendrimers,[10] cyclodextrins,[11] or micelles[12,13] have successfully been employed to enhance the control over factors such as the cargo loading capacity, retention time and release rates, and subsequent cell response. Liposomes, considered in biosensing[14] or as drug delivery vehicles,[15,16] have been used as components of multilayered films. However, so far their potential has largely been explored when assembled on colloidal templates in the form of capsosomes: (cargo-loaded) liposomes embedded within a polymer carrier capsule.[17,18] These assemblies have been used for encapsulated catalysis[19,20] or for the in vitro delivery of hydrophobic drugs to cancer cells.[21,22] On the other hand, while liposomes have been assembled together with polymer multilayers on planar substrates, either in the form of their aggregates[23] or via their anchoring to cholesterol-modified polymers,[24] their potential as drug deposits for surface-mediated drug delivery remains largely unexplored. The exceptions are a few reports including the demonstrated antibacterial activity of substrates containing silver nitrate loaded liposomes deposited within poly(L-lysine)/hyaluronic acid multilayers,[25] or the enzyme-triggered precipitation of calcium phosphates within liposomes in multilayered thin films.[26] Otherwise, planar substrates have mainly been used for the physical/chemical characterization of the film assembly and its properties.

Polydopamine (PDA) coatings have attracted considerable interests in the recent years as a simple and fast way to modify surfaces for biomedical applications. PDA is formed via a self-oxidative process of dopamine at mildly basic pH and is deposited on virtually any surface.[27] While the detailed polymerization mechanism and polymer structure remains to be identified,[28,29]

Received: March 22, 2011
Accepted: May 4, 2011
Published: May 04, 2011

Scheme 1. Schematic Illustration of Adsorption of Liposomes to PLL Precoated Glass Slides (i) Followed by the Deposition of a PDA Capping Layer (ii) and the Exposure of These Surfaces to Myoblast Cells (iii)

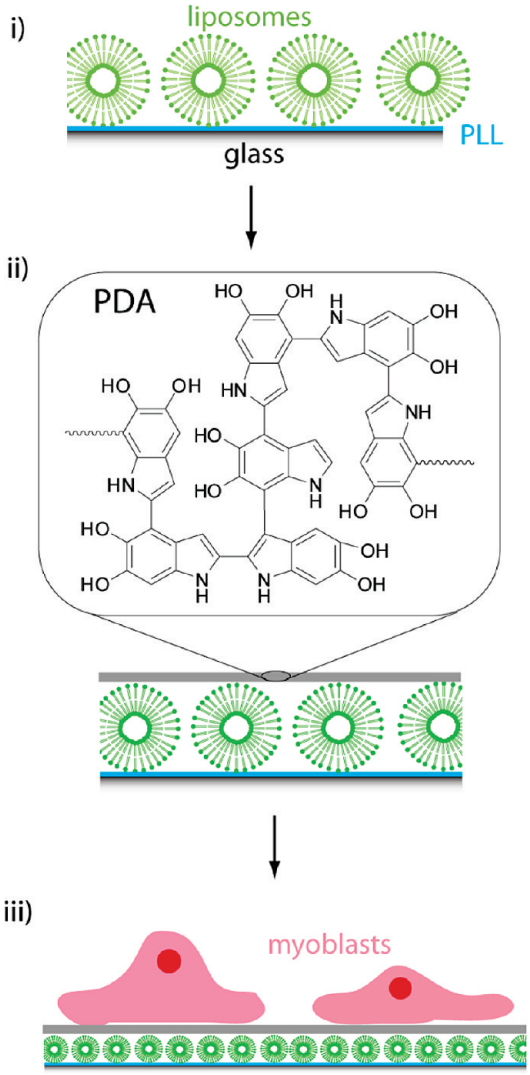

PDA coated surfaces are being explored for biosensing purposes[30,31] or to control cell adhesion to substrates.[32−34] PDA coatings represent a potentially interesting immobilization route for surface-mediated drug delivery. One recent report has explored this approach utilizing PDA as an adhesive layer to immobilize amphotericin B, a strong antifungal compound complexed to silica particles, on a glass slide, yielding antifungal surfaces.[35] However, no other work has explored PDA in the context of surface-mediated drug delivery.

Herein, we report the assembly of liposome/PDA surface coatings and their interaction with myoblast cells (Scheme 1). Specifically, we (i) determine the growth rate of PDA on glass, (ii) demonstrate that PDA allows adherence and proliferation of myoblasts, (iii) confirm that PDA is deposited on PLL/liposome coatings, and (iv) show the uptake of fluorescent lipids from the surface depending on the thickness of the PDA capping layer and the cell residence time. PDA is an attractive choice since, apart from its substrate independence and easy way of deposition, it also offers possibilities to covalently attach biomolecules, for example, specific antibodies, since postfunctionalization using amines or thiols is possible.[27] Liposomes on the other hand could serve as drug reservoirs since they are capable of entrapping small hydrophobic cargo and/or fragile biomolecules in a controlled manner. This report, for the first time, demonstrates the potential of liposomes as drug deposits embedded in PDA thin films for surface-mediated drug delivery.

EXPERIMENTAL SECTION

Materials. Poly(L-lysine) (PLL, M_w = 40 000−60 000), 4-(2-hydroxyethyl)piperazine-1-ethane-sulfonic acid (HEPES), tris-(hydroxymethyl)aminomethane (TRIS), sodium chloride (NaCl), ethanol, chloroform (pty ≥ 99.5%) and dopamine hydrochloride were purchased from Sigma-Aldrich. Zwitterionic 1,2-dioleoyl-*sn*-glycero-3-phosphocholine (DOPC, phase transition temperature −4 °C) and fluorescent lipids 1-oleoyl-2-[6-[(7-nitro-2−1,3-benzoxadiazol-4-yl)amino]hexanoyl]-*sn*-glycero-3phosphocholine (NBD-PC) were purchased from Avanti Polar Lipids, USA.

Two types of buffers were used throughout all of the experiments: HEPES buffer consisting of 10 mM HEPES and 150 mM NaCl (pH 7.4) and TRIS buffer consisting of 10 mM TRIS (pH 8.5). The buffer solutions were made with ultrapure water (Milli-Q gradient A 10 system, resistance 18 MΩ cm, TOC < 4 ppb, Millipore Corporation, USA).

Unilamellar liposome stock solutions were prepared by evaporation of the chloroform of 2.5 mg lipids under vacuum for 1 h, followed by hydration into 1 mL HEPES buffer and extrusion through 100 nm filters (11 times). For fluorescently labeled liposomes (L_{NBD}), 1 wt % of NBD-PC was added to the lipid mixture.

Substrate Modification. 18 × 18 mm^2 (cell experiments) or 9 mm diameter (XPS analysis) glass slides were cleaned via sonication in ethanol for 10 min, rinsed with ultrapure water, dried under nitrogen flow, and exposure to UV/ozone for 10 min.

PDA Coatings. The clean glass substrates were exposed to freshly prepared dopamine hydrochloride solution (5 mg mL^{-1} in TRIS buffer) for the required time. After the PDA deposition, the samples were rinsed with TRIS buffer and stored in HEPES buffer or rinsed with TRIS buffer and ultrapure water and dried under nitrogen flow for cell experiments and XPS analysis, respectively. Herein, PDA_x corresponds to a PDA coating with x min PDA polymerization time. Since the PDA not only is deposited onto surfaces but also forms PDA aggregates in solution, the solution was replaced if the PDA polymerization time was longer than 30 min to minimize the precipitation and adsorption of PDA aggregates formed in solution and to ensure continuous growth since depletion of the PDA concentration is unlikely to occur on this time scale and conditions.[36]

Liposome-Containing PDA Coatings. PLL (1 mg mL^{-1} in HEPES buffer, 10 min) was adsorbed as the precursor layer and rinsed with HEPES buffer. The samples were then exposed to an L (nonfluorescent liposomes) or L_{NBD} solution (stock solution 3 × diluted in HEPES buffer, 35 min), followed by rinsing in HEPES buffer. The PLL/L_{NBD} precoated substrates were exposed to a freshly prepared dopamine hydrochloride solution (5 mg mL^{-1} in TRIS buffer) for the required time to assemble the PDA capping layer. If PLL/$L_{(NBD)}$ precoated substrates required PDA layer with longer polymerization times, the dopamine hydrochloride solution was replaced every 30 min with fresh solution.

The coated substrates were stored in HEPES buffer for cell experiments or rinsed with ultrapure water and dried with nitrogen for XPS analysis.

Cell Work. The coated substrates were UV-sterilized for 1 h submerged in sterile HEPES buffer. The C2C12 mouse myoblast cell line (American Type Culture Collection) was used for all experiments. The cells (300 000 cells/flask in 40 mL medium) were cultured in 150 cm^2 culture flasks in medium (Dulbecco's modified Eagle's Medium with Glutamax (DMEM) supplemented with 10% fetal bovine serum, 50 U mL^{-1} penicillin, 50 μg mL^{-1} streptomycin, and 1 mM sodium pyruvate, all from Invitrogen) at 37 °C and 5% CO_2. The cells were seeded onto the substrates at a density of 100 000 cells/well in 3 mL medium and allowed to attach for different times at 37 °C and 5% CO_2. The samples were transferred into new wells to ensure that only the cells grown on the substrate are considered in the further analysis. The cells were washed 2 × with 3 mL PBS. 300 μL trypsin was used to detach the cells from the surface for the analysis by flow cytometry or the cells were fixed using 4% paraformaldehyde solution for 10 min followed by 3 washing steps in PBS for microscopy. All cell experiments were performed in at least three independent repeats.

Flow Cytometry. The cells grown on substrates coated with fluorescently labeled liposomes were analyzed using a C6 Flow Cytometer (Accuri Cytometers Inc.) and an excitation wavelength of λ = 488 nm. At least 3000 cells were analyzed.

Differential Interference Contrast (DIC) and Fluorescent Microscopy. DIC and fluorescent images of fixed cells were taken with a Zeiss inverted microscope equipped with a DIC slider, the corresponding filter sets and a 10× and a 40× objective. Prior to imaging, the substrates with the fixed cells were mounted on a glass cover slide using mounting media (Eukitt, Sigma).

X-ray Photoelectron Spectroscopy (XPS). XPS data acquisition was performed using a Kratos Axis Ultra^{DLD} instrument (Kratos Analytical Ltd., Telford, UK) equipped with a monochromated $Al_{k\alpha}$ X-ray source ($h\nu$ = 1486.6 electron volts, eV) operated at 15 kV and 15 mA (225 W). Survey spectra (binding energy (B.E.) range of 0−1100 eV with a pass energy of 160 eV) were acquired and analyzed using CasaXPS (Casa software Ltd.) software. The acquired data were converted to VAMAS format and analyzed using CASAXPS software.

RESULTS AND DISCUSSION

PDA Coatings. It is important to determine the PDA film thickness and the film growth rate for its use in surface-mediated drug delivery systems. Glass substrates were exposed to dopamine hydrochloride solutions for different times (up to 90 min) and the PDA coatings were analyzed by XPS. (A typical XPS survey scan can be found in Figure S1.) The thickness was quantified by determining the inelastic mean free path (IMFP) using the quantitative structure property relationships (QSPR) developed by Cumpson.[37] This method allows the IMFP to be estimated for any organic material from its chemical structure alone at the kinetic energy between ~200−2000 eV and the estimation is found to be more accurate than for other existing methods. By using QSPR, the IMFP of PDA at the energy of Si 2p photoelectron, $\lambda^{PDA/Si2p}$, is found to be 3.4 nm (more details regarding the calculation can be found in Supporting Information). The growth rate is further calculated by monitoring the attenuation of the Si 2p signal.[38] The PDA thickness and the growth rate is shown in Figure 1a. The growth was found to be linear with a growth rate of typically 3.6 nm per hour. This estimated growth rate is in agreement with the film thickness and the growth rate determined from the atomic force microscopy measurements by Postma et al.,[39] and was also confirmed by ellipsometry.[36] However, the estimated PDA thickness based

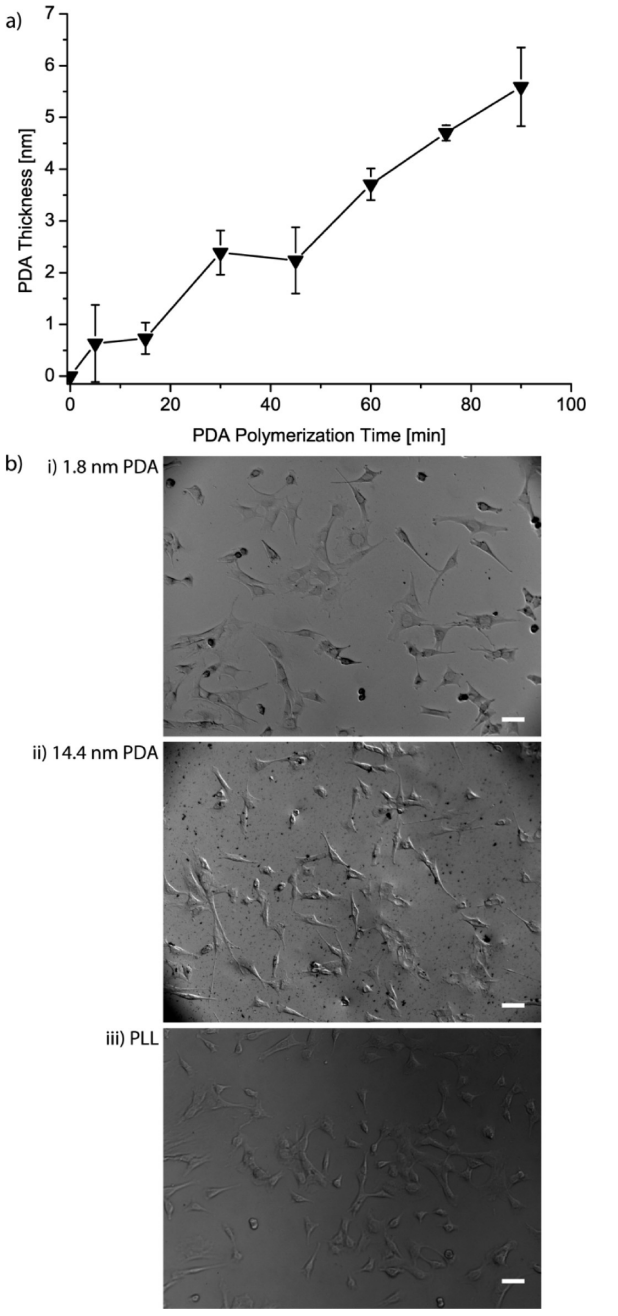

Figure 1. (a) PDA thickness on glass substrates depending on the PDA polymerization time as modeled from XPS data by applying the QSPR method. (b) Representative DIC images of fixed myoblast cells grown on glass substrates coated with PDA (i, ii) or PLL (iii) for 24 h. (i) PDA_{30} corresponds to a thickness of 1.8 nm, (ii) PDA thickness of 14.4 nm is an interpolated value corresponding to PDA_{240}. The scale bars correspond to 50 μm.

Table 1. Atomic Composition of Different Coatings Assembled on Glass Slides As Determined by XPS[a]

	atomic %			
coating	Si 2p	N 1s	O 1s	C 1s
glass	21.1 ± 0.1	0	64.9 ± 0.6	4.8 ± 0.4
glass/PLL/L	9.6 ± 2.3	2.4 ± 0.1	31.7 ± 6.5	50.6 ± 8.8
glass/PLL/L/PDA_{90}	2.8 ± 0.5	6.0 ± 1.0	18.6 ± 0.4	72.4 ± 0.01

[a] The decrease in substrate signal (Si 2p) and the simultaneous increase in N 1s confirms the assembly of the liposomes and suggests the deposition of the PDA capping layer. [b] Trace elements from the borosilicate glass observed including B, K, Ti, Na, Al, Zn, Cl. [c] Trace of P (typically less than 1%) observed for PLL/L and PLL/L/PDA_{90}.

on the XPS data in the latter report is different, mainly due to the fact that they use an IMFP of 3 nm, a value often applied for "common polymers".

To investigate if PDA coated surfaces support myoblasts adhesion and proliferation, cells were allowed to adhere to substrates coated either with PDA of different thicknesses (Figure 1bi and 1bii) or PLL (Figure 1biii) as control for 24 h. As examples, the cells grown on coatings of 1.8 nm PDA and 14.4 nm PDA are shown in the representative DIC images in Figure 1b. All the tested PDA coatings deposited with a polymerization time between 5 and 300 min were supporting cell adhesion and proliferation to the same extent, making PDA a promising coating for this cell type.

Liposome-Containing PDA Coatings. The potential use of the PDA coatings with liposomes as drug deposits was explored. While we have previously shown that intact liposomes are adsorbed to PLL coated surface,[24] the polymerization of PDA on substrates precoated with PLL/L has never been reported before and was characterized using XPS. (A typical XPS survey scan can be found in Supporting Information Figure S2.) Contrary to a single layer system such as PDA on glass, determining the growth rate of PDA on a multilayered system is found to be complex, thus have not been attempted in this study. The IMFP values for each component within the multilayer system are expected to be different and the behavior of each layer upon exposure to the ultra high vacuum condition is unknown, thus determining the PDA thickness solely from the attenuation of the Si 2p signal would be inaccurate. Nevertheless, to confirm that the PDA coating is indeed forming on the upper most layer, the attenuation of Si 2p from the glass substrate should be observed with each layer deposition step. The atomic composition of the major peaks (Si 2p, C 1s, O 1s, N 1s) were compared for a clean glass slide, and glass slides coated with PLL/L and PLL/L/PDA_{90} (Table 1). With each additional deposition step, the substrate signal (Si 2p) is decreasing, from 21.1% for a clean glass slide to 2.8% for the PLL/L/PDA_{90} coating, suggesting that the film thickness is increasing. In parallel, the N 1s signal is increasing with each deposition step. While no nitrogen was detected on a clean glass slide, PLL/L and PLL/L/PDA_{90} coatings have shown a subsequent increase in N 1s because of the nitrogen in PLL and the liposomes as well as in PDA. The combination of these two results strongly suggests that the PDA is deposited. However, the detected substrate signal (Si 2p) remained rather large for PLL/L/PDA_{90} coatings, suggesting that there could be surface dewetting and/or that the PDA growth on PLL/L precoated substrates is slower than on glass.

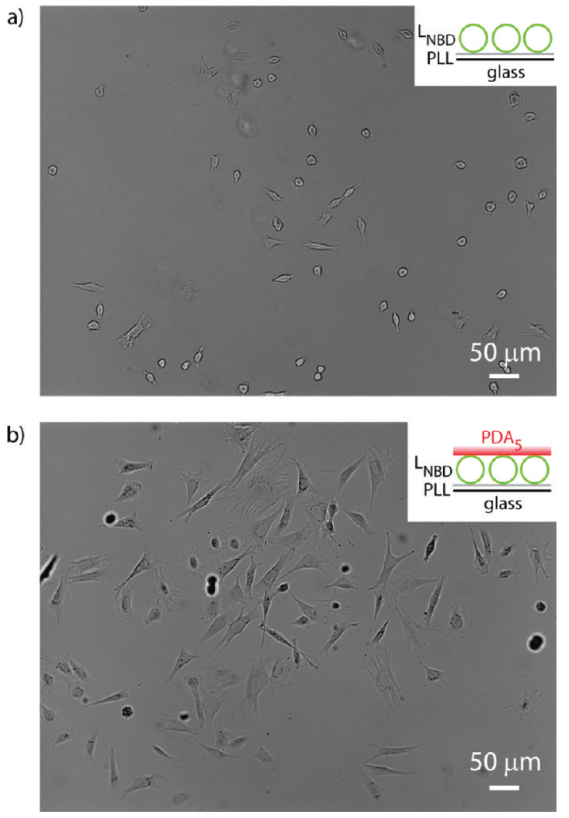

Figure 2. Representative DIC images of myoblasts let to adhere for 4 h on a glass substrate coated with PLL/L_{NBD} (a) or PLL/L_{NBD}/PDA_5 (b), showing that even this short polymerization time is turning the surface cell adhesive.

PDA coatings containing fluorescent liposome were exposed to myoblasts for 4 h with the aim to assess the cell adhesion to these substrates in comparison to PLL and PLL/L_{NBD} coated glass slides. While PLL allows cells to spread (Figure 1biii), substrates coated with PLL/L_{NBD} were far less able to supporting cell adhesion (Figure 2a). However, even a very thin PDA capping layer (5 min PDA polymerization time) on the liposomes made these substrates cell adhesive (Figure 2b). Further, all the other tested PLL/L_{NBD}/PDA_x coated substrates supported myoblast adhesion and proliferation.

Surface-mediated drug delivery requires the uptake of the therapeutics from the substrate. With the aim to proof the concept that hydrophobic cargo embedded within the lipid bilayer of the liposomes can be internalized by myoblasts from the surface, fluorescent lipids as part of the lipid membrane of L_{NBD} were employed, and the fluorescent intensities of cells were characterized by flow cytometry. Further, an expected route to control the uptake efficiency is via the thickness of the PDA capping layer. To this end, the PDA polymerization time was varied and the myoblasts were allowed to adhere for 4 h to the different substrates. The results are summarized in Figure 3a with the dashed line referring to the autofluorescent level of cells grown on a PLL coated substrate. First, with increasing PDA polymerization time, the fluorescent intensity of the cells started to drop, with PDA_{300} almost completely hindering the fluorescent lipid association with the cells within 4 h. Interestingly, although PDA coatings adsorbed for 5 min are supporting cell adhesion equally well than PDA coatings deposited for 30 min, the fluorescent intensity of the cells in the first case is lower. We

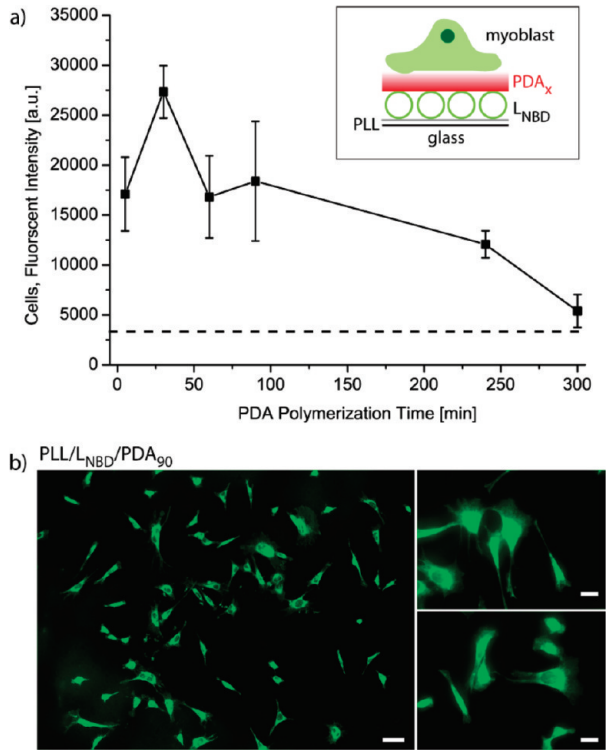

Figure 3. (a) Fluorescent intensity of myoblasts as measured by flow cytometry is shown. Prior to harvesting for the flow cytrometry measurements, the cells adhered for 4 h to substrates coated with PLL/L_{NBD} capped with a PDA layer deposited with different polymerization times. The dashed line corresponds to the autofluorescence of cells grown on a PLL coated surface. (b) Representative fluorescent microscopy images of fixed myoblasts grown for 4 h on a glass slide coated with PLL/L_{NBD}/PDA_{90}. The green fluorescence of the cells, which is localized around the nuclei, is due to the uptake of the fluorescent lipids from the surface. The scale bar in the left image corresponds to 50 μm and to 20 μm in the two right ones.

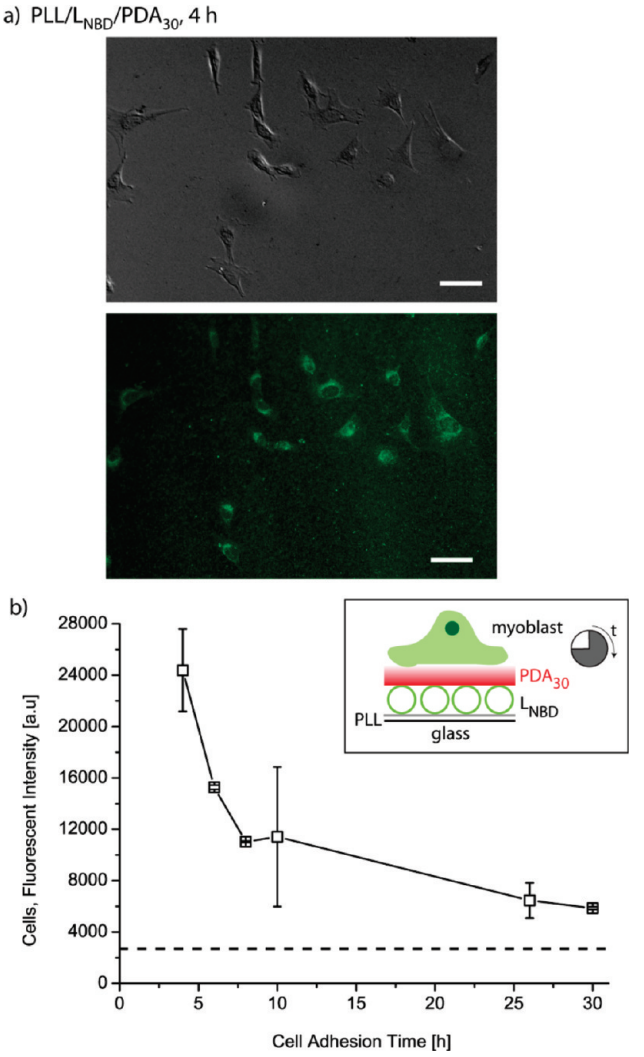

Figure 4. (a) Representative DIC and fluorescent microscopy images of myoblasts adhering to PLL/L_{NBD}/PDA_{30} for 4 h. The green background in the bottom image is due to the immobilized fluorescent liposomes. The fluorescence of the cells is due to the internalized fluorescent lipids. The scale bars correspond to 50 μm. (b) The fluorescent intensity of myoblasts as measured by flow cytometry is shown. Prior to harvesting for the flow cytrometry measurements, the cells adhered to substrates coated with PLL/L_{NBD}/PDA_{30} for different time points. The dashed line corresponds to the autofluorescence of cells grown on a PLL coated surface.

hypothesize that the liposomes in this case are less protected. Components of the cell medium might start degrading them, such that they are lost from the surface and unavailable for the cells. Further, flow cytometry revealed that all the cells in the population were similarly fluorescent, suggesting that the surface was homogenously coated with liposomes. The representative fluorescent microscopy images in Figure 3b show myoblast cells after 4 h adhering to a PLL/L_{NBD}/PDA_{90} coated surface. The fluorescence of the cells is due to the uptake of the fluorescent lipids from the surface. The entire cells became fluorescent with the highest intensity located in the close proximity of the nuclei (see close ups on the right). This is a particularly interesting finding and could proof very valuable when delivery of cargo to the nuclei using liposomes as drug deposits in polymer thin films is considered in the future.

With the aim to get a first insight into how long the liposomes on the surface are available for the cells, the dependence of the fluorescent lipid uptake on the cell residence time on an exemplary coating (PLL/L_{NBD}/PDA_{30}) was assessed. Figure 4a shows a representative DIC and fluorescent microscopy image of the cells after 4 h. While the green background demonstrated the presence of the liposomes, it also makes the capturing of an image of the fluorescent cells more difficult. The fluorescence of myoblasts grown on this coating was measured at different time points by flow cytometry (Figure 4b). After 8 h of cell residence time, the fluorescent intensity of the cells was 50% lower as it was after 4 h. During the subsequent 22 h, their fluorescent intensity is further reduced, almost down to the autofluorescent level of the cells. There are three possible explanations: (a) the proliferating cells are depleting the liposomes on the surface, (b) the internalized fluorescent lipids are passed on during cell division and this is diluting the fluorescence per cell, or (c) the cells are processing the fluorescent lipids. Currently, we can not yet pinpoint the details of the uptake process or if one or more of the above-mentioned options are more likely to occur, but our findings open up an entirely new avenue of drug delivery concepts, which could be explored.

CONCLUSION

Herein, we demonstrated a linear growth rate for PDA on glass substrates and that these coatings supported the adherence and proliferation of myoblast cells. Further, we showed that PDA capping layers can be deposited on PLL/L precoated substrates and by doing so, the surfaces became cell adhesive. A model compound, that is, fluorescent lipids were taken up from the surface by these cells, demonstrated by the increased fluorescence of the cells. Thicker PDA coatings led to lower fluorescent intensity of the cells, suggesting that the uptake could be controlled via the polymerization time of the PDA capping layer. Cells with increasing residence time on PLL/L_{NBD}/PDA_{30} coated substrates had reduced fluorescent intensity, probably either due to depletion of the liposomes on the surface by the proliferating cells or due to the fluorescent lipids being processed by the cells.

Taken together, we report a surface modification approach which has the potential to deliver cargo from the surface using liposomes as deposits, which offer themselves as carrier for hydrophobic and hydrophilic drugs. Further, multilayers of liposomes could be considered to control the amount and release rate of delivered therapeutics but also the codelivery of different active cargo could be envisioned.

ASSOCIATED CONTENT

Supporting Information. Detailed calculation of the inelastic mean free path (IMFP) and typical XPS survey scans. This material is available free of charge via the Internet at http://pubs.acs.org.

AUTHOR INFORMATION

Corresponding Author
*E-mail: bstadler@inano.au.dk.

ACKNOWLEDGMENT

This work was supported by the Lundbeck foundation, Denmark, and a Sapere Aude Starting Grant from the Danish Council for Independent Research, Technology and Production Sciences, Denmark.

REFERENCES

(1) Zelikin, A. N. *ACS Nano* **2010**, *4*, 2494–2509.
(2) Harnet, J. C.; Le Guen, E.; Ball, V.; Tenenbaum, H.; Ogier, J.; Haikel, Y.; Vodouhe, C. *J. Mater. Sci.: Mater. Med.* **2009**, *20*, 185–193.
(3) Vodouhe, C.; Le Guen, E.; Garza, J. M.; Francius, G.; Dejugnat, C.; Ogier, J.; Schaaf, P.; Voegel, J. C.; Lavalle, P. *Biomaterials* **2006**, *27*, 4149–4156.
(4) Pavlukhina, S.; Lu, Y. M.; Patimetha, A.; Libera, M.; Sukhishvili, S. *Biomacromolecules* **2010**, *11*, 3448–3456.
(5) Crouzier, T.; Ren, K.; Nicolas, C.; Roy, C.; Picart, C. *Small* **2009**, *5*, 598–608.
(6) Mac Donald, M. L.; Rodriguez, N. M.; Shah, N. J.; Hammond, P. T. *Biomacromolecules* **2010**, *11*, 2053–2059.
(7) Mac Donald, M. L.; Samuel, R. E.; Shah, N. J.; Padera, R. F.; Beben, Y. M.; Hammond, P. T. *Biomaterials* **2011**, *32*, 1446–1453.
(8) Zhang, J. T.; Montanez, S. I.; Jewell, C. M.; Lynn, D. M. *Langmuir* **2007**, *23*, 11139–11146.
(9) Saurer, E. M.; Yamanouchi, D.; Liu, B.; Lynn, D. M. *Biomaterials* **2011**, *32*, 610–618.
(10) Nguyen, P. M.; Zacharia, N. S.; Verploegen, E.; Hammond, P. T. *Chem. Mater.* **2007**, *19*, 5524–5530.
(11) Smith, R. C.; Riollano, M.; Leung, A.; Hammond, P. T. *Angew. Chem., Int. Ed.* **2009**, *48*, 8974–8977.
(12) Kim, B. S.; Park, S. W.; Hammond, P. T. *ACS Nano* **2008**, *2*, 386–392.
(13) Kim, B. S.; Smith, R. C.; Poon, Z.; Hammond, P. T. *Langmuir* **2009**, *25*, 14086–14092.
(14) Bally, M.; Bailey, K.; Sugihara, K.; Grieshaber, D.; Vörös, J.; Städler, B. *Small* **2010**, *6*, 2481–2497.
(15) Sawant, R. R.; Torchilin, V. P. *Soft Matter* **2010**, *6*, 4026–4044.
(16) Torchilin, V. P. *Adv. Drug Delivery Rev.* **2006**, *58*, 1532–1555.
(17) Chong, S. F.; Chandrawati, R.; Stadler, B.; Park, J.; Cho, J. H.; Wang, Y. J.; Jia, Z. F.; Bulmus, V.; Davis, T. P.; Zelikin, A. N.; Caruso, F. *Small* **2009**, *5*, 2601–2610.
(18) Städler, B.; Chandrawati, R.; Goldie, K.; Caruso, F. *Langmuir* **2009**, *25*, 6725–6732.
(19) Chandrawati, R.; Hosta-Rigau, L.; Vanderstraaten, D.; Lokuliyana, S. A.; Städler, B.; Albericio, F.; Caruso, F. *ACS Nano* **2010**, *4*, 1351–1361.
(20) Städler, B.; Chandrawati, R.; Price, A. D.; Chong, S. F.; Breheney, K.; Postma, A.; Connal, L. A.; Zelikin, A. N.; Caruso, F. *Angew. Chem., Int. Ed.* **2009**, *48*, 4359–4362.
(21) Hosta-Rigau, L.; Chandrawati, R.; Saveriades, E.; Odermatt, P. D.; Postma, A.; Ercole, F.; Breheney, K.; Wark, K. L.; Städler, B.; Caruso, F. *Biomacromolecules* **2010**, *11*, 3548–3555.
(22) Hosta-Rigau, L.; Städler, B.; Yan, Y.; Nice, E. C.; Heath, J. K.; Albericio, F.; Caruso, F. *Adv. Funct. Mater.* **2010**, *20*, 59–66.
(23) Volodkin, D. V.; Schaaf, P.; Mohwald, H.; Voegel, J. C.; Ball, V. *Soft Matter* **2009**, *5*, 1394–1405.
(24) Chandrawati, R.; Städler, B.; Postma, A.; Connal, L. A.; Chong, S. F.; Zelikin, A. N.; Caruso, F. *Biomaterials* **2009**, *30*, 5988–5998.
(25) Malcher, M.; Volodkin, D.; Heurtault, B.; Andre, P.; Schaaf, P.; Mohwald, H.; Voegel, J. C.; Sokolowski, A.; Ball, V.; Boulmedais, F.; Frisch, B. *Langmuir* **2008**, *24*, 10209–10215.
(26) Michel, M.; Arntz, Y.; Fleith, G.; Toquant, J.; Haikel, Y.; Voegel, J. C.; Schaaf, P.; Ball, V. *Langmuir* **2006**, *22*, 2358–2364.
(27) Lee, H.; Dellatore, S. M.; Miller, W. M.; Messersmith, P. B. *Science* **2007**, *318*, 426–430.
(28) Ito, S.; Wakamatsu, K. *Photochem. Photobiol.* **2008**, *84*, 582–592.
(29) d'Ischia, M.; Napolitano, A.; Pezzella, A.; Meredith, P.; Sarna, T. *Angew. Chem., Int. Ed.* **2009**, *48*, 3914–3921.
(30) Fu, Y. C.; Li, P. H.; Bu, L. J.; Wang, T.; Xie, Q. J.; Xu, X. H.; Lei, L. H.; Zou, C.; Yao, S. Z. *J. Phys. Chem. C* **2010**, *114*, 1472–1480.
(31) Ouyang, R. Z.; Lei, J. P.; Ju, H. X. *Nanotechnology* **2010**, *21*, 185502–185510.
(32) Bettinger, C. J.; Bruggeman, P. P.; Misra, A.; Borenstein, J. T.; Langer, R. *Biomaterials* **2009**, *30*, 3050–3057.
(33) Ku, S. H.; Lee, J. S.; Park, C. B. *Langmuir* **2010**, *26*, 15104–15108.
(34) Ku, S. H.; Ryu, J.; Hong, S. K.; Lee, H.; Park, C. B. *Biomaterials* **2010**, *31*, 2535–2541.
(35) Paulo, C. S. O.; Vidal, M.; Ferreira, L. S. *Biomacromolecules* **2010**, *11*, 2810–2817.
(36) Bernsmann, F.; Ponche, A.; Ringwald, C.; Hemmerle, J.; Raya, J.; Bechinger, B.; Voegel, J. C.; Schaaf, P.; Ball, V. *J. Phys. Chem. C* **2009**, *113*, 8234–8242.
(37) Cumpson, P. J. *Surf. Interface Anal.* **2001**, *31*, 23–34.
(38) Ratner, B. D.; Castner, D. G. In *Surface Analysis—The Principal Techniques*; 2nd ed.; Vickerman, J. C., Gilmore, I. S., Eds.; **2009**; pp 47−112.
(39) Postma, A.; Yan, Y.; Wang, Y. J.; Zelikin, A. N.; Tjipto, E.; Caruso, F. *Chem. Mater.* **2009**, *21*, 3042–3044.